Cancer Research

Improving Drug Penetrability with iRGD Leverages the Therapeutic Response to Sorafenib and Doxorubicin in Hepatocellular Carcinoma

Christian Schmithals[1], Verena Köberle[1], Hüdayi Korkusuz[2], Thomas Pleli[1], Bianca Kakoschky[1], Eduardo Alonso Augusto[1], Ahmed Atef Ibrahim[1,3], Jose M. Arencibia[1], Vida Vafaizadeh[4], Bernd Groner[4], Horst-Werner Korf[5], Bernd Kronenberger[1], Stefan Zeuzem[1], Thomas J. Vogl[6], Oliver Waidmann[1], and Albrecht Piiper[1]

Abstract

iRGD is a derivative of the integrin-binding peptide RGD, which selectively increases the penetrability of tumor tissue to various coadministered substances in several preclinical models. In this study, we investigated the ability of iRGD to improve the delivery of sorafenib and doxorubicin therapy in hepatocellular carcinoma (HCC) using established mouse models of the disease. A contrast-enhanced MRI method was developed in parallel to assess the *in vivo* effects of iRGD in this setting. We found that iRGD improved the delivery of marker substances to the tumors of HCC-bearing mice about three-fold without a parallel increase in normal tissues. Control peptides lacking the critical CendR motif had no effect. Similarly, iRGD also selectively increased the signal intensity from tumors in Gd-DTPA–enhanced MRI. In terms of antitumor efficacy, iRGD coadministration significantly augmented the individual inhibitory effects of sorafenib and doxorubicin without increasing systemic toxicity. Overall, our results offered a preclinical proof of concept for the use of iRGD coadministration as a strategy to widen the therapeutic window for HCC chemotherapy, as monitored by Gd-DTPA–enhanced MRI as a noninvasive, clinically applicable method to identify iRGD-reactive tumors. *Cancer Res; 75(15); 3147–54. ©2015 AACR.*

Downloaded from http://aacrjournals.org/cancerres/article-pdf/75/15/3147/2719066/3147.pdf by guest on 14 December 2024

Introduction

Hepatocellular carcinoma (HCC) is the third ranking cause of cancer-related mortality and is highly resistant to anticancer drugs (1, 2). In the majority of cases, HCC is diagnosed in advanced stages. Therefore, only a minority of patients has potentially curative treatment options, including radiofrequency ablation, resection, and liver transplantation. Patients with advanced unresectable or metastatic disease have a median survival of only a few months, which can be extended by the multikinase inhibitor sorafenib by 2 to 3 months, but at the expense of substantial side effects (3). Thus, there is a strong clinical need to improve the drug therapy of patients with HCC.

A selective increase of the delivery of systemically administered anticancer drugs into the HCCs would be an important step toward improving the efficacy of the therapy in this tumor entity. Recently, pioneering work from Ruoslahti and colleagues has shown that particular peptides containing a vascular recognition motif, an R/KXXR/K tissue penetration (CendR) motif, and a protease recognition site, increase the delivery of diverse kinds of attached reagents such as nanoparticles, viruses, or antibodies in several mouse tumor models, taking payloads deep into tumor tissue, whereas normal tissues remain unaffected (4, 5). These peptides, prototypically represented by the cyclic RGD peptide CRGDK/RGPD/EC, termed iRGD, home to the tumors by initially binding to α_v integrins that are specifically expressed on the endothelium of tumor vessels and other cells within the tumors, but not in normal tissues, and are then cleaved by an unknown protease (4–7). This results in the generation of CRGDK/R, which dissociates from the integrins and binds to neuropilin-1 (NRP1), thereby activating an endocytic bulk transport pathway through the tumor tissue (8–11). The increased tumor delivery of iRGD-conjugated payloads has been shown in different experimental tumor models by other independent studies (12, 13) and translates into a higher therapeutic efficacy (4, 5).

iRGD can also increase the concentrations of diverse systemically administered substances specifically in tumors, when coadministered rather than being directly coupled to the cargo in some tumor models (5, 14, 15). This bystander effect of iRGD would be much more convenient and versatile, as it would allow combined application with the currently used antitumor drugs but is less well-investigated than its transport-enhancing effect upon coupling to the cargo and thus needs validation and examination in

[1]Department of Medicine 1, University Hospital Frankfurt, Frankfurt, Germany. [2]Department of Nuclear Medicine, University Hospital Frankfurt, Frankfurt, Germany. [3]The Immunology and Infectious Diseases Laboratory, Therapeutic Chemistry Department, The National Research Center, Dokki, Cairo, Egypt. [4]Georg-Speyer Haus, Frankfurt am Main, Germany. [5]Institute of Anatomy 2, University Hospital Frankfurt, Frankfurt, Germany. [6]Department of Diagnostic and Interventional Radiology, University Hospital Frankfurt, Frankfurt, Germany.

Note: Supplementary data for this article are available at Cancer Research Online (http://cancerres.aacrjournals.org/).

Corresponding Author: Albrecht Piiper, Department of Medicine 1, University Hospital Frankfurt/M., Theodor-Stern-Kai 7, D-60590 Frankfurt, Germany. Phone: 49-69-6301-87667; Fax: 49-69-6301-87689; E-mail: piiper@med.uni-frankfurt.de

doi: 10.1158/0008-5472.CAN-15-0395

©2015 American Association for Cancer Research.

other tumor entities. Moreover, the effect of iRGD on tumor penetrability is likely to vary among different tumors, for instance, due to differential expression of $\alpha_v\beta_{3/5}$ integrins and NRP1 (14). Thus, for an efficient use of iRGD, a clinically applicable method to determine whether a particular tumor reacts to iRGD would be highly beneficial.

iRGD has not been explored in HCC. In particular, the bystander effect of iRGD would be of high clinical importance in this tumor entity, as it could be used to increase the therapeutic index of sorafenib in HCC, and it may confer therapeutic efficacy to antitumor substances that are not beneficial to the patients *per se*. Here, we show that iRGD shows the bystander effect in HCC mouse models, that the increased tumor-penetrability by iRGD can be detected by Gd-DTPA-enhanced MRI with and without iRGD, and that iRGD augments the therapeutic effects of coadministered sorafenib and doxorubicin.

Materials and Methods

Peptides

Synthetic iRGD (CRGDKGPDC) and RGD control peptide (CRGDDGPKC), synthesized circular via a cystein–cystein disulfide bond between amino acid 1 and 9 (5), were purchased from GenScript USA Inc. The purity was more than 98%.

Generation of transgenic mice and visualization of HCC

All animal experiments were approved by the local animal care committee and were in agreement with German legal requirements. The animals were inspected every 2 to 3 days. Male TGFα/c-myc bitransgenic mice were generated by crossing homozygous metallothionein/TGFα and albumin/c-myc single transgenic mice in CD13B6CBA background as described (16, 17). After weaning, the mice received $ZnCl_2$ (via the drinking water) to induce the expression of TGFα and thereby accelerate hepatocarcinogenesis. To detect and monitor the endogenously formed HCCs in the TGFα/c-myc mice, gadoxetic acid (Gd-EOB-DTPA)-enhanced MRI was performed on a 3T MRI scanner (Siemens Magnetom Trio, Siemens Medical Solutions) as described recently (17–19). A representative image of HCC imaging by Gd-EOB-DTPA–enhanced MRI is shown in Supplementary Fig. S1. Mice with HCC as visualized by Gd-EOB-DTPA–enhanced MRI were used in the subsequent experiments.

Nude mice experiments

HepG2 and Huh-7 cells were obtained from ATCC and RIKEN BioResource Center, respectively, and were grown in DMEM supplemented with 10% FBS and penicillin/streptomycin (Life Technologies; ref. 17). The cells were authenticated by SNP genotyping within the past 6 months and were routinely monitored for morphologic and growth characteristics and mycoplasms. A total of 5×10^6 cells (resuspended in 100 μL of PBS) was injected subcutaneously into the flanks of NMRI Foxn1 nude mice (Harlan Laboratories B.V.). Three to 4 weeks later, the mice were assigned to the treatment groups. For the tumor penetration experiments, the mice were used 5 to 7 weeks after the inoculation of the tumor cells.

Tumor penetration experiments

TGFα/c-myc mice with liver tumors according to Gd-EOB-DTPA–enhanced MRI or nude mice bearing HepG2 and Huh-7 xenografts received iRGD, RGD control peptide (4 μmol/kg each), or PBS by tail vein injection. Fifteen minutes later, Evans Blue (33.3 mg/kg, MP Biomedicals) or doxorubicin (20 mg/kg, Sigma-Aldrich) was injected intravenously. Another 30 (Evans Blue) or 60 minutes (doxorubicin) later, the mice were terminally perfused with Ringer solution by cannulation of the left heart ventricle. After laparotomy, the organs were inspected macroscopically, and the liver, tumor, and other organs were excised. For Evans Blue quantification, the dye was extracted from tissues in *N*,*N*-dimethylformamide for 24 hours at 37°C and quantified by measuring the absorbance at 600 nm with a spectrophotometer (Beckman Coulter, DU 800).

To determine the concentration of doxorubicin in the organs, the tissues were homogenized in 1% SDS and 1 mmol/L H_2SO_4 in water. Thereafter, doxorubicin was extracted by adding 2 mL of chloroform/isopropanol (1:1, v/v) to the homogenized samples, followed by vortexing and freeze/thaw cycles. The samples were centrifuged at $14{,}000 \times g$ for 15 minutes, and the absorbance of the organic phase (lowest phase) at 490 nm was measured photometrically.

Gd-DTPA–enhanced MRI with and without iRGD

To study the effect of iRGD on Gd-DTPA–enhanced MRI of HCC, TGFα/*c-myc* mice, in which HCC had been detected by Gd-EOB-DTPA–enhanced MRI one week before or nude mice with HepG2 or Huh-7 were used. The mice were anesthetized by intraperitoneal injection of ketamine (70mg/kg body weight) and xylazine (10 mg/kg body weight), followed by a basal T1–weighted MRI and immediately thereafter a Gd-DTPA–enhanced MRI (17). Twelve to 24 hours later, either iRGD or RGD control peptide (100 μL each via tail vein) was injected, followed by a basal and a Gd-DTPA–enhanced MRI (18). For quantitative analyses of the MRI data, signal intensities were measured with operator-defined regions of interest (ROI) drawn into the images as described recently (19). ROIs were placed in livers and tumors. Signal intensity changes were calculated by subtracting the precontrast values from the signal intensities obtained upon addition of Gd-DTPA. The alterations of the signal intensity in the tumors and livers due to iRGD or RGD control peptide were expressed as fold increase of the signal intensity by Gd-DTPA preinjected with PBS.

Treatment of nude mice

Doxorubicin was dissolved in PBS and sorafenib in a vehicle containing 12.5% Cremophor and 12.5% ethanol. Nude mice bearing HepG2 or Huh-7 xenografts received iRGD, RGD control peptide (4 μmol/kg by tail vein injection), or PBS 15 minutes each time before treatment with doxorubicin (3 mg/kg, 3 times per week intraperitoneally) or sorafenib (every second day orally). Body weight and tumor size were determined every 2 to 3 days with a caliper. At the end of the experiment, the mice were sacrificed by cervical dislocation. Tumors were excised and weighed.

Phospho-kinase array

Tumor homogenates were analyzed in a panel of phosphorylation profiles of kinases (Human Phospho-MAPK Array, ARY002B; R&D Systems). The tumor lysates were matched for protein as determined by the BCA protein assay (BioRad). Each membrane was incubated with 200 μg of protein lysates as described by the manufacturer. A cocktail of biotinylated detection antibodies, streptavidin–horseradish peroxidase and chemiluminescent detection reagents were used to detect the phosphorylated

Downloaded from http://aacrjournals.org/cancerres/article-pdf/75/15/3147/2719066/3147.pdf by guest on 14 December 2024

proteins. The relative amount of the specific phosphorylated proteins was determined following quantification of scanned images by Image-Pro plus program.

Statistical analysis

Data are expressed as means ± SD or SEM as indicated. Comparisons were performed with Mann–Whitney *U* (Kruskal–Wallis) or Student *t* test. $P < 0.05$ was considered significant and is one-sided. Data were analyzed using the BiAS software for Windows (version 9.11, Epsilon-Verlag).

Results

Coadministered iRGD, but not a peptide containing an RGD motif lacking CendR motif, increases the entry of Evans Blue and doxorubicin selectively in HCC

To investigate whether iRGD shows the bystander effect in HCC, we examined the effect of intravenously administered iRGD on the levels of coadministered albumin-binding dye Evans Blue in TGFα/c-myc mice with endogenously formed HCC (16). To this end, mice with liver tumors as detected by Gd-EOB-DTPA–enhanced MRI were intravenously injected with iRGD, an RGD peptide lacking the CendR motif (RGD control peptide) or saline, followed by intravenous administration of Evans Blue 15 minutes later. After another 30 minutes, the mice were terminally perfused. Photometric quantification of the dye extracted from the tissues revealed a 3-fold increase of Evans Blue in the tumor tissue from iRGD-injected mice as compared with the HCC tissue from PBS-injected mice ($P = 0.014$ as compared with RGD control peptide and $P = 0.0012$ as compared with PBS), whereas the RGD control peptide or vehicle had no effect (Fig. 1A). iRGD or control peptide had no effects on the concentration of Evans Blue in the normal tissues examined (liver, kidney, spleen, and lung), indicating that iRGD specifically increased the permeability of the HCC tissue in TGFα/c-myc mice for codelivered substances.

To examine whether the bystander effect of iRGD also occurs in HCC xenograft mouse models, we studied the effect of intravenously injected iRGD on the levels of systemically administered Evans Blue in nude mice bearing HepG2 or Huh-7 xenografts. iRGD increased the levels of coadministered Evans Blue in HepG2 and Huh-7 xenografts by 3.4-fold ($P \leq 0.002$; HepG2 cells) and 2.6-fold ($P < 0.001$; Huh-7 cells), respectively, as compared with the tumors from animals treated with PBS or RGD control peptide (Fig. 1B and C).

Next, we investigated the influence of iRGD on the tissue concentrations of intravenously coadministered doxorubicin, a therapeutic substance, which can be tracked by its fluorescence, in the TGFα/c-myc and HepG2 xenograft HCC mouse models. As illustrated in Fig. 2, iRGD increased the levels of doxorubicin in the HCCs of both HCC models ($P \leq 0.0011$). In contrast, iRGD had no effect on the doxorubicin levels in other organs (Fig. 2A). The control peptide had no effect on the levels of doxorubicin in any tissue examined. Thus, iRGD strongly and selectively increased the levels of doxorubicin in the HCC tissue in 2 HCC mouse models.

Coadministered iRGD selectively increases the signal intensity of HCC in Gd-DTPA–enhanced MRI

A potentially clinically applicable method to determine whether iRGD causes permeabilization of a given tumor would be highly beneficial, for example, before a therapeutic application

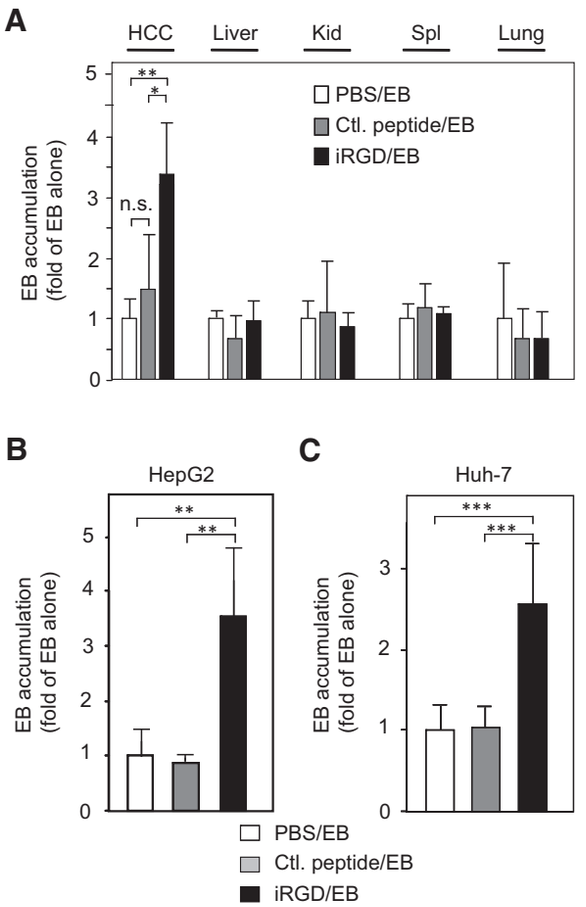

Figure 1.
Coadministered iRGD, but not a peptide containing a RGD motif lacking the CendR motif, increases entry of Evans Blue (EB) selectively in HCC tissue in TGFα/c-myc mice as well as in two HCC xenografts in nude mice. TGFα/c-myc mice bearing MRI-verified liver tumors (A) or mice bearing subcutaneous HepG2 (B) or Huh-7 xenografts (C) were intravenously injected with 4 μmol/kg of iRGD or control peptide (dissolved in PBS), or PBS alone, followed 5 minutes later by 1 mg of Evans Blue. Tissues were collected 30 minutes later. Evans Blue accumulation in tumor and liver tissues of the mice was quantified. Values are means ± SD; $n = 4$–5. Asterisks indicate a significant difference (*, $P < 0.05$; **, $P < 0.01$; ***, $P < 0.001$). n.s., not significant.

of iRGD. Therefore, we examined whether the tumor-permeabilizing effect of iRGD can be detected by Gd-DTPA–enhanced MRI, a broadly used clinical procedure, in TGFα/c-myc mice with endogenously formed HCCs as detected by Gd-EOB-DTPA–enhanced MRI one week before. These mice were subjected to a Gd-DTPA–enhanced MRI, which showed negatively contrasted HCCs in the livers (Fig. 3B, left). Twelve to 24 hours later, the mice were injected with iRGD or RGD control peptide, followed by Gd-DTPA–enhanced MRI (Fig. 3A). As illustrated in Fig. 3B (left), the tumors in the mice injected with PBS or RGD control peptide were negatively contrasted in the livers. Injection of iRGD before the Gd-DTPA–enhanced MRI elicited a substantial increase in the signal intensity of the tumors, which now were positively rather than negatively contrasted in the livers (Fig. 3B, right). In contrast, iRGD and RGD control peptide did not alter the signal intensity of liver or other normal tissues, suggesting specificity of this effect of

Downloaded from http://aacrjournals.org/cancerres/article-pdf/75/15/3147/2719066/3147.pdf by guest on 14 December 2024

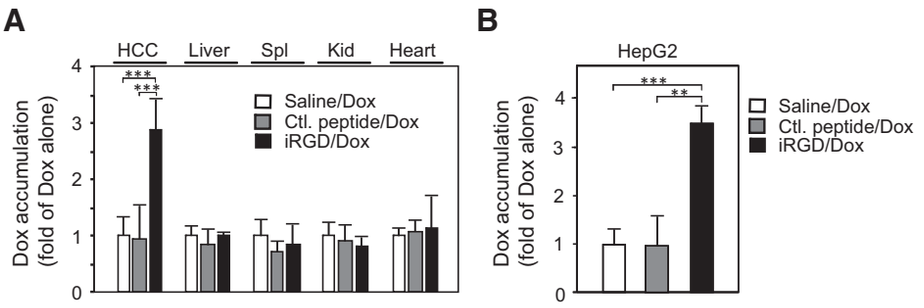

Figure 2.
Coadministered iRGD increased the entry of doxorubicin selectively in HCC tissue from TGFα/c-myc mice and HepG2 xenografts. TGFα/c-myc mice with MRI-verified liver tumors (A) or nude mice bearing subcutaneous HepG2 xenografts (B) were intravenously injected with 4 μmol/kg of iRGD or control (Ctl.) peptide in PBS or PBS alone, followed 10 minutes later by doxorubicin (Dox; 20 mg/kg). Tissues were collected 30 minutes later. Doxorubincin accumulation in tumor tissue as well as other tissues of the mice was quantified. Values are means ± SD; $n = 5$–6. Asterisks indicate a significant difference (**, $P < 0.01$; ***, $P < 0.001$). Kid, kidney; Spl, spleen.

iRGD for the tumors. Quantitative densitometric analyses of the signal intensities revealed a 2-fold increase in the tumors upon injection of iRGD as compared with the injection of RGD control peptide ($P = 0.004$) or PBS ($P < 0.001$; Fig. 3C). The response of the HCCs to iRGD showed some variance in the transgenic HCC mouse model, ranging from substantial increase in signal intensity in approximately half of the tumors, whereas others responded less or not at all, reflecting heterogeneity of the tumors in this HCC mouse model.

We next investigated whether iRGD also increased the MRI signal of the tumors in HCC xenograft–bearing nude mice. As shown in Fig. 3D, iRGD effectively increased the signal intensity of the tumors in the HepG2 tumors ($P = 0.0311$). Similar observations were obtained in Huh-7 xenografts ($P = 0.0081$), but the increase of the tumor signal was less pronounced (1.5-fold; Fig. 3E) as compared with the other HCC mouse models (≤2-fold). These data indicate that the iRGD-induced increase in tumor penetrability could be detected noninvasively by Gd-DTPA–enhanced MRI in the 3 different HCC mouse models.

iRGD increased the therapeutic effect of doxorubicin as well as of sorafenib in HepG2 tumor–bearing nude mice

We next examined whether the iRGD-induced increase of the HCC penetrability is accompanied by an increased efficacy of therapeutic substances in HCC. Although the response rates to doxorubicin as single agent are low and prolonged survival of the patients with advanced HCC could not be demonstrated (20, 21), it is possible that elevated intratumoral doxorubicin levels upon coinjection of iRGD may translate into an increased therapeutic response to doxorubicin. Therefore, we studied the effect of coadministered iRGD on tumor progression in nude mice bearing established HepG2 xenografts. The animals were treated with iRGD, control peptide or PBS, and doxorubicin. The progression of HepG2 xenografts was significantly reduced in mice treated with doxorubicin and iRGD as compared with those treated with doxorubicin and control peptide (Fig. 4A). At the end of the experiment, the tumor volumes from the mice treated with iRGD and doxorubicin had increased by approximately 50%, whereas those in mice treated with doxorubicin plus control peptide showed a 3-fold increase ($P = 0.0061$; Fig. 4A). Accordingly, the tumor masses were significantly lower in mice treated with iRGD plus doxorubicin as compared with those from mice treated with doxorubicin and control peptide ($P = 0.035$) or PBS ($P = 0.0027$; Fig. 4B). The body weight shift was similar, irrespective of whether doxorubicin was given alone or in combination with iRGD (Supplementary Fig. S2). This supports the notion that the elevated antitumor effect of the combination therapy as compared with doxorubicin alone was due to increased intratumoral doxorubicin levels and inhibition of tumor growth rather than an increased toxicity.

Sorafenib is the only drug currently approved that prolongs survival of patients with advanced HCC (3). However, a major portion of patients does not respond to sorafenib therapy and substantial side effects are frequent (3). To investigate whether iRGD may improve the therapeutic efficacy of sorafenib in HCC, HepG2 xenograft–bearing nude mice were treated with iRGD and a low dose of sorafenib (20 mg/kg every second day) or vehicle. Sorafenib alone or in combination with control peptide produced small growth-inhibitory effects, which did not reach statistical significance. In contrast, in mice treated with sorafenib plus iRGD, tumor progression was significantly reduced as compared with mice treated with sorafenib alone ($P = 0.014$ at the end of the experiment) or sorafenib plus control peptide ($P = 0.001$ at the end of treatment; Fig. 4C). Determination of the tumor masses at the end of the experiment revealed that the tumors from iRGD-plus sorafenib-treated animals had significantly lower masses than the tumors from animals treated with sorafenib alone ($P < 0.001$) or with control peptide plus sorafenib ($P = 0.011$; Fig. 4D). Similar results were obtained in Huh-7 xenografted nude mice (Fig. 4E and F). The body weight shifts were the same irrespective of whether sorafenib was given alone or combined with iRGD (Supplementary Fig. S3), indicating that iRGD increased the therapeutic efficacy of sorafenib without increasing its toxicity.

To investigate whether coadministered iRGD indeed acts by reinforcing the inhibitory effects of sorafenib on intracellular kinase pathways, we studied the relative phosphorylation levels of major families of mitogen-activated protein kinases (MAPK) and other signal transduction regulators in the HepG2 tumors from the mice treated with vehicle, sorafenib, or sorafenib plus iRGD. Tumors from animals treated with sorafenib alone showed a significant decrease in phosphorylation only in a small number of proteins as compared with tumors from vehicle-treated mice (JNK, p38γ, Creb, and AKT3; Supplementary Fig. S4). In contrast,

Downloaded from http://aacrjournals.org/cancerres/article-pdf/75/15/3147/2719066/3147.pdf by guest on 14 December 2024

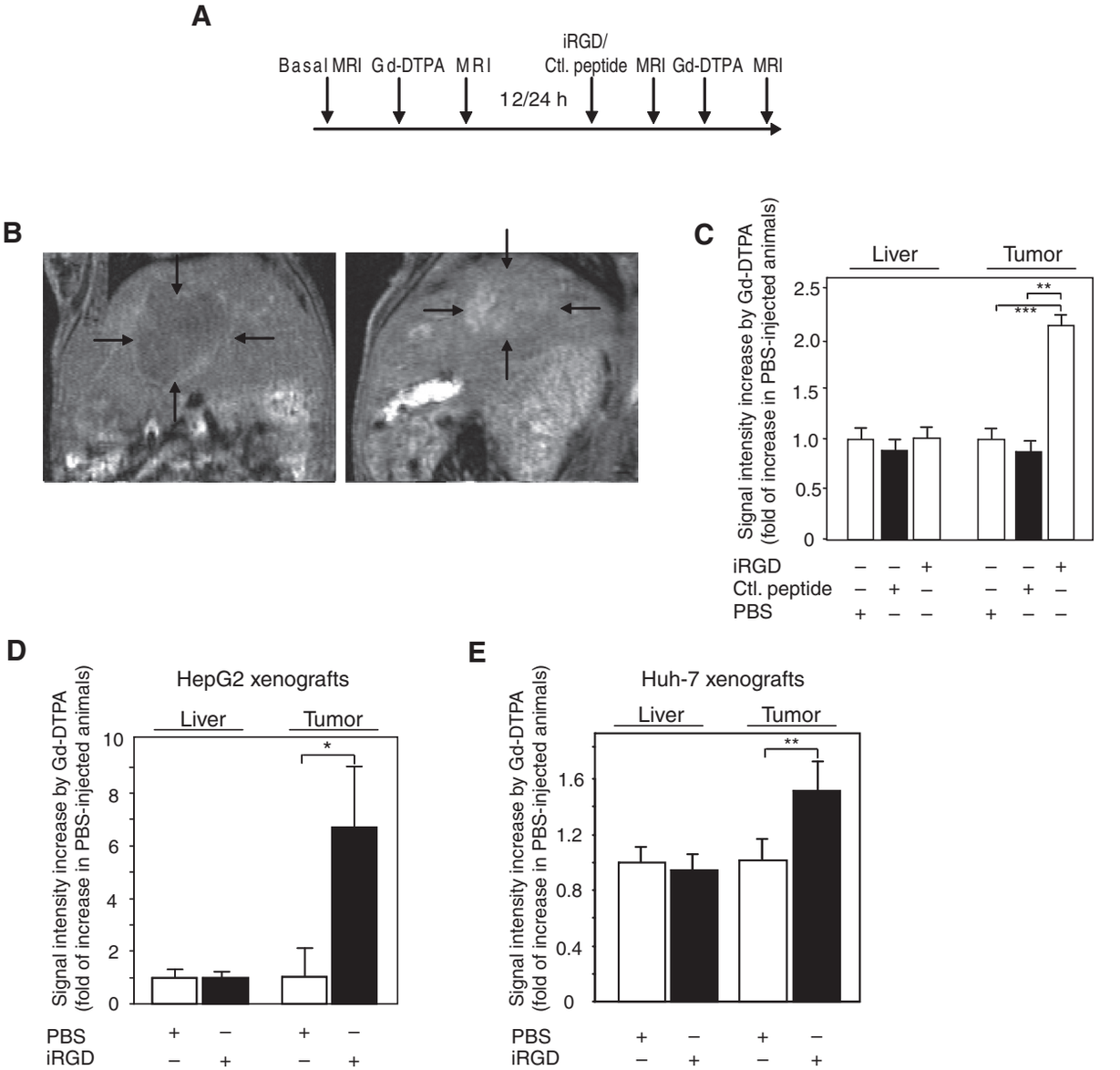

Figure 3.
iRGD led to a tumor-specific increase of signal intensity in Gd-DTPA–enhanced MRI. TGFα/*c-myc* mice, in which HCC had been detected 1 week before by Gd-EOB-DTPA–enhanced MRI, were anesthetized, followed by a basal T1–weighted MRI and immediately thereafter a Gd-DTPA–enhanced MRI. Twelve to 24 hours later, either iRGD or RGD control (Ctl.) peptide (100 μL each via the tail vein containing 4 μmol/kg) was injected into the same animals, followed by a basal and a Gd-DTPA–enhanced MRI. A, schematic outline of the procedure. B, Gd-DTPA–enhanced MRI of a TGFα/c-myc mice with HCC (left), followed by the injection of iRGD and another Gd-DTPA–enhanced MRI 12 hours later. Arrows mark the tumor. C, quantitative analyses of the MRI data. Values are means ± SD; $n = 12$. D, twelve animals with HepG2 xenografts were injected on day 1 with control peptide, followed by a Gd-DTPA–enhanced MRI. On the next day, the animals were injected with iRGD, followed by a Gd-DTPA–enhanced MRI. Values are means ± SEM. E, thirteen animals with Huh-7 xenografts were subjected to the same procedure as in D. Values are means ± SEM. Asterisks indicate significant differences (*, $P < 0.05$; **, $P < 0.01$; ***, $P < 0.001$).

in tumors from animals cotreated with sorafenib and iRGD, the inhibitory effect of sorafenib on kinase phosphorylation was increased and reached significance for most detected proteins as compared with the vehicle-treated tumors. Only RSK1 and mitogen-activated protein kinase kinase 3 (MKK3) were not altered by the sorafenib treatment, regardless the presence of iRGD. Creb was inhibited to the same extent by iRGD/sorafenib and sorafenib only (Supplementary Fig. S4B). Overall, including iRGD significantly reduced the phosphorylation of 15 of 24 proteins (Supplementary Fig. S4B). These results indicate that coadministered iRGD reinforced the inhibitory effect of sorafenib on intracellular signaling kinases and are in good agreement with the effects of sorafenib and sorafenib plus iRGD on the progression of the HepG2 tumors.

Downloaded from http://aacrjournals.org/cancerres/article-pdf/75/15/3147/2719066/3147.pdf by guest on 14 December 2024

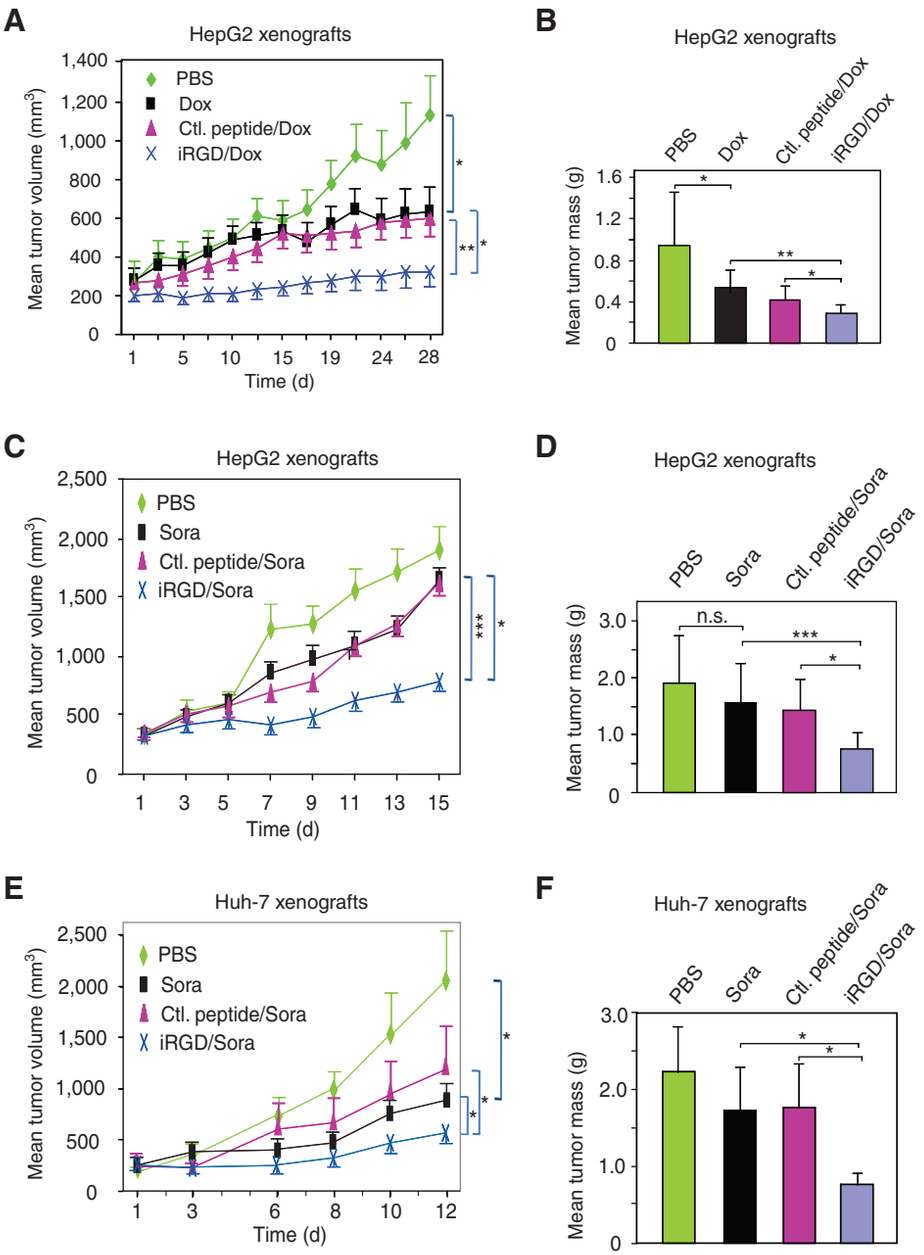

Figure 4.
iRGD augmented the tumor growth inhibitory effect of sorafenib and doxorubicin in nude mice bearing HCC xenografts. A and B, HepG2 tumor xenograft–bearing nude mice were injected with 4 μmol/kg of iRGD or control (Ctl.) peptide or PBS intravenously 15 min before the administration of doxorubicin (Dox; 3 mg/kg three times per week intraperitoneally). The volume of the tumors (A) and the tumor masses at the end of the experiment (B) were measured ($n = 7$–11). Values are means ± SD. C and D, HepG2 tumor xenograft–bearing mice received 4 μmol/kg of iRGD or control (Ctl.) peptide or PBS (i.v.) 15 minutes before the administration of sorafenib (Sora; 20 mg/kg every second day orally). The volume of the tumors (C) and the tumor masses at the end of the experiment (D) were measured ($n = 10$–11). E and F, Huh-7 tumor xenografted nude mice received 4 μmol/kg of iRGD or control (Ctl.) peptide or PBS (i.v.) 15 minutes before the administration of sorafenib (30 mg/kg every second day orally). The volume of the tumors (E) and the tumor masses at the end of the experiment (F) were measured ($n = 6$–14). Values are means ± SEM. Asterisks indicate a significant differences (*, $P < 0.05$; **, $P < 0.01$; ***, $P < 0.001$). n.s., not significant.

Discussion

A selective increase of the tumor penetrability by iRGD might be highly beneficial in tumor therapy, as it could be used to achieve a tumor-selective delivery of intravenously coadministered antitumor substances, thereby increasing the therapeutic index. We found that iRGD increased the levels of the coinjected marker substances doxorubicin or Evans Blue in the tumor tissue of TGFα/c-myc mice with endogenously formed HCCs as well as in HepG2 and Huh-7 xenograft–bearing nude mice by a factor of 3 without changing the levels of these substances in normal tissues. This suggests that iRGD selectively increased the delivery of coadministered substances into HCC tissue in the different HCC mouse models. In other tumor models, this has been shown to occur through an increased penetrability of the tumor stroma, enabling systemically administered substances to penetrate deeply into the tumor (4, 5). It appears likely that this also applies to HCC. The bystander effect of iRGD appears to avoid many of the drawbacks of other strategies to increase the concentration of anticancer drugs selectively in tumor tissue such as the enhanced permeability and retention (EPR) effect or active targeting by harnessing tumor-specific surface molecules, such as large tumor-to-tumor variability, often low efficacy and specificity, restriction to a particular class of substances and tumors, or low capacity (22, 23). iRGD is well-tolerated in all studies published so far and even inhibits tumor metastasis (10). Moreover, iRGD may enable the penetration of systemically coadministered substances into fibrotic areas in breast carcinoma xenografts (24). As HCCs arise in the predominant number of cases in livers with advanced fibrosis or

Downloaded from http://aacrjournals.org/cancerres/article-pdf/75/15/3147/2719066/3147.pdf by guest on 14 December 2024

cirrhosis (2), iRGD might be particularly useful to increase tumor drug delivery in this tumor entity.

The efficacy of iRGD to increase the penetrability of tumors for therapeutic substances is likely to show tumor-to-tumor variation, which could be, for instance, due to differential expression of $\alpha_v\beta_{3/5}$ integrins and NRP1 (14). Thus, a clinically feasible method to determine whether a particular tumor can be permeabilized by iRGD would be highly beneficial for a potential translation of iRGD into patients. Our data showing that intravenously administered iRGD led to a selective increase of the MRI signal in the tumors, leading to a conversion of otherwise negatively contrasted tumors to positively contrasted ones in Gd-DTPA–enhanced MRI injected in the TGFα/c-myc mice, indicates that the increased tumor penetrability due to the action of iRGD could be detected *in vivo* noninvasively by Gd-DTPA–enhanced MRI, a clinical routine procedure. Thus, Gd-DTPA–enhanced MRI with and without iRGD may offer a clinically applicable new method to examine whether a particular tumor responds to iRGD and may thus enable optimization of drug administration regimen. Moreover, an altered behavior in Gd-DTPA–enhanced MRI upon administration of iRGD might serve as a new selective identifier for malignant liver lesions.

Another key finding of the present study is that the tumor-permeabilizing effect of iRGD translates into an enhanced antitumor effect of sorafenib, the current standard drug in patients with advanced HCC. Whereas sorafenib alone at the relatively low-dose schedule used in the present study (to minimize toxicity) had only little, if any, effect on tumor progression, it strongly reduced HCC progression when administered in combination with iRGD. There was no indication that iRGD increased the toxicity of sorafenib, suggesting that iRGD may indeed increase the therapeutic index of sorafenib. iRGD is well-tolerated in other preclinical tumor models (5, 9) and currently awaits entering early clinical testing. Moreover, considering that RGD peptides have low immunogenicity, the accumulated data indicate that the combined administration of iRGD and sorafenib might be highly beneficial in HCC.

Considering the conservation of the effect of iRGD in different human tumor xenograft and spontaneous mouse tumor models (5) and the expression of the α_v integrin and NRP1 in the vessels and the tumor cells of human HCC (6, 25–29), it appears possible that the enhanced tumor penetrability to the drugs due to the action of iRGD described in the present study in HCC mouse models may translate to patients with HCC. However, this remains to be investigated. If this would be the case, patients with HCC may benefit from an increased efficacy of the sorafenib therapy in several ways. iRGD may augment the antitumor effect of sorafenib and prolong patient survival as compared with the patients treated with sorafenib alone; coadministered iRGD may increase the portion of patients responding to the sorafenib therapy. Moreover, iRGD may allow a reduction of the dose of sorafenib, resulting in diminishing the considerable side effects of this drug.

Coadministered iRGD also increased the antitumor effect of doxorubicin in HCC mice. There was no sign that iRGD increased the toxicity of doxorubicin. This is in agreement with other studies showing that iRGD did not increase the cardiotoxicity of doxorubicin (5), the main dose-limiting toxicity of doxorubicin. If the tumor-permeabilizing effect of iRGD also holds for patients with HCC, it is possible that doxorubicin, although not beneficial in patients with HCC as single agent (20, 21), might be effective in patients with HCC when administered with iRGD.

It should be noted that many aspects and details concerning the action of iRGD and its use of Gd-DTPA–enhanced MRI for the detection of the tumor-penetrating effect of iRGD will need further experimentation. For instance, the efficacy of combinations of iRGD with antitumor drugs might be further improved by optimization of the peptide (30), dosing and administration regimen, the identification of particularly effective combinations, and a comparison of the effect of iRGD on Gd-DTPA–enhanced MRI and transport of the marker substances in the same animals would enable more exact estimation of the suitability of MRI to detect iRGD-responsive tumors.

In summary, the present study not only shows that the bystander effect of iRGD extends to HCC. We also show that the increased penetrability of the HCCs by iRGD can be detected by a noninvasive clinical routine imaging procedure and results in a higher therapeutic efficacy of coadministered drugs. These findings render clinical development of iRGD for HCC and potentially other tumors highly attractive.

Disclosure of Potential Conflicts of Interest

No potential conflicts of interest were disclosed.

Authors' Contributions

Conception and design: C. Schmithals, V. Köberle, B. Groner, B. Kronenberger, S. Zeuzem, O. Waidmann, A. Piiper

Development of methodology: C. Schmithals, H.-W. Korf, A. Piiper

Acquisition of data (provided animals, acquired and managed patients, provided facilities, etc.): C. Schmithals, V. Köberle, T. Pleli, B. Kakoschky, E.A. Augusto, A.A. Ibrahim, V. Vafaizadeh, B. Groner, H.-W. Korf, B. Kronenberger, T.J. Vogl

Analysis and interpretation of data (e.g., statistical analysis, biostatistics, computational analysis): C. Schmithals, V. Köberle, H. Korkusuz, T. Pleli, B. Kakoschky, E.A. Augusto, A.A. Ibrahim, H.-W. Korf, B. Kronenberger, O. Waidmann, A. Piiper

Writing, review, and/or revision of the manuscript: C. Schmithals, V. Köberle, J.M. Arencibia, B. Groner, H.-W. Korf, B. Kronenberger, S. Zeuzem, O. Waidmann, A. Piiper

Administrative, technical, or material support (i.e., reporting or organizing data, constructing databases): S. Zeuzem

Study supervision: B. Kronenberger, S. Zeuzem, A. Piiper

Acknowledgments

The authors thank S.S. Thorgeirsson and E.A. Conner (Laboratory of Experimental Carcinogenesis, Center for Cancer Research, National Cancer Institute, NIH, Bethesda, MD) for kindly providing c-myc and TGFα transgenic mice, and K. Breuhahn (Department of Pathology, University of Heidelberg, Heidelberg, Germany) for support.

Grant Support

This work was supported by grants from the GRK1172 (DFG and Merck KGaA, Germany), a grant from the University Hospital Frankfurt (Dr. Paul und Cilli Weil-Stiftung, Heinrich und Fritz Riese-Stiftung), and the Scholari Foundation.

The costs of publication of this article were defrayed in part by the payment of page charges. This article must therefore be hereby marked *advertisement* in accordance with 18 U.S.C. Section 1734 solely to indicate this fact.

Received February 12, 2015; revised April 27, 2015; accepted May 18, 2015; published online August 1, 2015.

Downloaded from http://aacrjournals.org/cancerres/article-pdf/75/15/3147/2719066/3147.pdf by guest on 14 December 2024

References

1. Jemal A, Bray F, Center MM, Ferlay J, Ward E, Forman D. Global cancer statistics. CA Cancer J Clin 2011;61:69–90.
2. Hernandez-Gea V, Toffanin S, Friedman SL, Llovet JM. Role of the microenvironment in the pathogenesis and treatment of hepatocellular carcinoma. Gastroenterology 2013;144:512–27.
3. Llovet JM, Ricci S, Mazzaferro V, Hilgard P, Gane E, Blanc JF, et al. SHARP Investigators Study Group. Sorafenib in advanced hepatocellular carcinoma. N Engl J Med 2008;359:378–90.
4. Sugahara KN, Teesalu T, Karmali PP, Kotamraju VR, Agemy L, Girard OM, et al. Tissue-penetrating delivery of compounds and nanoparticles into tumors. Cancer Cell 2009;16:510–20.
5. Sugahara KN, Teesalu T, Karmali PP, Kotamraju VR, Agemy L, Greenwald DR, et al. Coadministration of a tumor-penetrating peptide enhances the efficacy of cancer drugs. Science 2010;328:1031–5.
6. Desgrosellier JS, Cheresh DA. Integrins in cancer: biological implications and therapeutic opportunities. Nat Rev Cancer 2010;10:9–22.
7. Ruoslahti E. Specialization of tumour vasculature. Nat Rev Cancer 2002;2:83–99.
8. Teesalu T, Sugahara KN, Kotamraju VR, Ruoslahti E. C-end rule peptides mediate neuropilin-1-dependent cell, vascular, and tissue penetration. Proc Natl Acad Sci USA 2009;106:16157–62.
9. Teesalu T, Sugahara KN, Ruoslahti E. Tumor-penetrating peptides. Front Oncol 2013;3:216.
10. Sugahara KN, Braun GB, de Mendoza TH, Kotamraju VR, French RP, Lowy AM, et al. Tumor-penetrating iRGD peptide inhibits metastasis. Mol Cancer Ther 2015;14:120–8.
11. Pang HB, Braun GB, Friman T, Aza-Blanc P, Ruidiaz ME, Sugahara KN, et al. An endocytosis pathway initiated through neuropilin-1 and regulated by nutrient availability. Nat Commun 2014;5:4904.
12. Puig-Saus C, Rojas LA, Laborda E, Figueras A, Alba R, Fillat C, et al. iRGD tumor-penetrating peptide-modified oncolytic adenovirus shows enhanced tumor transduction, intratumoral dissemination and antitumor efficacy. Gene Ther 2014;21:767–74.
13. Zhu Z, Xie C, Liu Q, Zhen X, Zheng X, Wu W, et al. The effect of hydrophilic chain length and iRGD on drug delivery from poly(ε-caprolactone)-poly (N-vinylpyrrolidone) nanoparticles. Biomaterials 2011;32:9525–35.
14. Akashi Y, Oda T, Ohara Y, Miyamoto R, Kurokawa T, Hashimoto S, et al. Anticancer effects of gemcitabine are enhanced by co-administered iRGD peptide in murine pancreatic cancer models that overexpressed neuropilin-1. Br J Cancer 2014;110:1481–7.
15. Kadonosono T, Yamano A, Goto T, Niibori M, Kuchimaru T, Kizaka-Kondoh S. Cell penetrating peptides improve tumor delivery of cargos through neuropilin-1-dependent extravasation. J Control Release 2015; 201C:14–21.
16. Murakami H, Sanderson ND, Nagy P, Marino PA, Merlino G, Thorgeirsson SS. Transgenic mouse model for synergistic effects of nuclear oncogenes and growth factors in tumorigenesis: interaction of c-myc and transforming growth factor α in hepatic oncogenesis. Cancer Res 1993;53:1719–23.
17. Haupenthal J, Bihrer V, Korkusuz H, Kollmar O, Schmithals C, Kriener S, et al. Reduced efficacy of the Plk1 inhibitor BI 2536 on the progression of hepatocellular carcinoma due to low intratumoral drug levels. Neoplasia 2012;14:410–9.
18. Watcharin W, Schmithals C, Pleli T, Köberle V, Korkusuz H, Hübner F, et al. Detection of hepatocellular carcinoma in transgenic mice by Gd-DTPA- and rhodamine 123-conjugated human serum albumin nanoparticles in T1 magnetic resonance imaging. J Control Release 2015;199:63–71.
19. Korkusuz H, Ulbrich K, Welzel K, Koeberle V, Watcharin W, Bahr U, et al. Transferrin-coated gadolinium nanoparticles as MRI contrast agent. Mol Imaging Biol 2013;15:148–54.
20. Yau T, Chan P, Epstein R, Poon RT. Management of advanced hepatocellular carcinoma in the era of targeted therapy. Liver Int 2009;29:10–17.
21. Asghar U, Meyer T. Are there opportunities for chemotherapy in the treatment of hepatocellular cancer? J Hepatol 2012;56:686–95.
22. Ruoslahti E, Bhatia SN, Sailor MJ. Targeting of drugs and nanoparticles to tumors. J Cell Biol 2010;188:759–68.
23. Chauhan VP, Jain RK. Strategies for advancing cancer nanomedicine. Nat Mater 2013;12:958–62.
24. Chen R, Braun GB, Luo X, Sugahara KN, Teesalu T, Ruoslahti E. Application of a proapoptotic peptide to intratumorally spreading cancer therapy. Cancer Res 2013;73:1352–61.
25. Pellet-Many C, Frankel P, Jia H, Zachary I. Neuropilins: structure, function and role in disease. Biochem J 2008;411:211–26.
26. Nejjari M, Hafdi Z, Gouysse G, Fiorentino M, Béatrix O, Dumortier J, et al. Expression, regulation, and function of alpha V integrins in hepatocellular carcinoma: an *in vivo* and *in vitro* study. Hepatology 2002;36:418–26.
27. Bergé M, Allanic D, Bonnin P, de Montrion C, Richard J, Suc M, et al. Neuropilin-1 is upregulated in hepatocellular carcinoma and contributes to tumour growth and vascular remodelling. J Hepatol 2011;55: 866–75.
28. Edwards S, Lalor PF, Tuncer C, Adams DH. Vitronectin in human hepatic tumours contributes to the recruitment of lymphocytes in an $\alpha v\beta 3$-independent manner. Br J Cancer 2006;95:1545–54.
29. Dong YW, Wang R, Cai QQ, Qi B, Wu W, Zhang YH, et al. Sulfatide epigenetically regulates miR-223 and promotes the migration of human hepatocellular carcinoma cells. J Hepatol 2014;60:792–801.
30. Pang HB, Braun GB, She ZG, Kotamraju VR, Sugahara KN, Teesalu T, et al. A free cysteine prolongs the half-life of a homing peptide and improves its tumor-penetrating activity. J Control Release 2014;175:48–53.

Downloaded from http://aacrjournals.org/cancerres/article-pdf/75/15/3147/2719066/3147.pdf by guest on 14 December 2024